

Nanostructure Formation and Phase Separation in Surfactant Solutions

Sanat K. Kumar

*Department of Materials Science and Engineering,
Pennsylvania State University, University Park, PA 16802.*

M. Antonio Floriano

*Department of Chemistry, Università della Calabria,
87036 Arcavacata di Rende (CS), Italy*

Athanasios Z. Panagiotopoulos [†]

*Department of Chemical Engineering,
Princeton University, Princeton NJ 08544-5263*

Abstract

We have studied the phase and micellization behavior of a series of model surfactant systems using Monte Carlo simulations on cubic lattices of coordination number $z=26$. The phase behavior and thermodynamic properties were studied through the use of histogram reweighting methods, and the nanostructure formation studied through examination of the behavior of the osmotic pressure as a function of composition, and through analysis of configurations. Our results show that only phase separation occurs for the surfactants with short head groups. Nanostructure formation then occurs for long head groups or for short heads where these moieties repel each other strongly. The transition from phase separation to nanostructure formation is thus quasi-continuous, and can be readily tuned by varying surfactant architecture and interactions. The results obtained from these simulations, which can be qualitatively understood through theories valid for block copolymers in selective solvents, provide the first benchmark studies against which analytical theories can be compared.

[†]To whom correspondence should be addressed. Electronic mail: azp@princeton.edu

I. INTRODUCTION

Surfactant molecules are well known to spontaneously assemble into many different nanostructures, e.g., micelles, bilayers and vesicles [1–4]. The competition between the propensity of the head group(s) for the solvent, and the tendency of hydrocarbon tails to minimize solvent contact dictate the equilibrium structure. Previous *analytical* work in this area has stressed the importance of various microscopic parameters, including the sizes of the hydrocarbon tails and the head groups, as well as the interaction energies between these different species. Israelachvili [5] derived criteria for the shapes assumed by nanostructures based on packing arguments on the hydrocarbon tails in the surfactant assembly. The central parameter in this development is the dimensionless ratio:

$$\Delta \equiv \frac{v}{a_0 l_c} \quad (1)$$

where v is the hydrocarbon volume, and l_c the maximum extension of the hydrocarbon tail. a_0 is the optimal surface area per head, which is generally different from its geometric area a . For $\Delta \leq 1/3$, spherical micelles are predicted to form, cylindrical micelles are predicted for $1/3 < \Delta \leq 1/2$, and bilayers for $\Delta > 1/2$. While these relationships are quite useful, unfortunately, they require knowledge of the optimal area per head group which is only normally known by examining the resulting structure. Consequently, it has been common practice to replace a_0 by a , the geometric area of the head group. As we have shown in previous work [6], and as we shall show below, this often results in qualitatively incorrect predictions for the nanostructures adopted by these surfactants in solution.

Typical time scales for formation of micellar aggregates in solution are tens to hundreds of μs [7]. Because these time scales are much longer than those that can be covered in a simulation of an atomistically detailed model, simulation studies of self-assembly are performed using simplified models, either in the continuum [8] or, more commonly, on lattices [9–12].

In past work, we have begun to investigate systematically the factors controlling the self assembly of amphiphilic molecules utilizing Monte Carlo simulations on a lattice [6, 13]. We have shown that thermodynamic properties obtained from relatively small systems,

can pinpoint the critical micelle concentration. This fact circumvents another problem encountered in typical simulations, where a large number of molecules have to be considered to observe the formation of enough micelles to obtain accurate averages. In our notation H denotes the “water soluble” (hydrophilic) head moieties, while T the tail (hydrophobic) groups. The phase behavior and self assembly of symmetric surfactants H_3T_3 and H_4T_4 were studied by grand canonical Monte Carlo simulations which were able to determine the solubility limits of the surfactants as well as their aggregation behavior. The critical micelle concentration was shown to be accompanied by a change in slope of a plot of the osmotic pressure vs. surfactant concentration, thus suggesting that micellization was accompanied by changes in thermodynamic properties. However, micellization is not a true thermodynamic transition, due to the finite size of the structures which result.

We have reanalyzed the data presented in [6] and found that, for H_4T_4 , Δ changes from a value of 0.25 at $T^*=6$ to a value of 0.19 at $T^*=8$, which is close to the upper micellization temperature. These results are consistent with the observations that these surfactants yield spherical nanostructures. However, note that this parameter alone is insufficient to anticipate the fact that for $T^* > 8.5$ no coherent micelles form.

In this context we note that the formation of nanostructures by amphiphilic molecules represents a careful balance between the “solvophobic” and “solvophilic” interactions. A dominance of either can lead to either phase separation or complete solubility of the amphiphile in the solvent. While the subtle balance between these forces are recognized in the current literature, the crossover from one behavior to the next remains to be understood in a quantitative fashion.

To gain more insights into the micellization processes, and the competition between phase separation and self assembly, here we report Monte Carlo results for surfactant molecules with asymmetric chemical structures. We start with pure T molecules, which phase separate from solvent but show no self assembly, and progressively increase the length of the H block. Self assembly occurs before phase separation for longer H blocks and we find, progressively, the occurrence of worm like micelles and spherical micelles as the H length is increased.

II. SIMULATION DETAILS

A Models and Methods

Short diblock and triblock surfactants of structure H_xT_y and $T_xH_yT_x$ were studied on cubic lattices of coordination number $z=26$. This lattice model for surfactants was originally proposed by Larson [14–16], and used by us previously. The lattice consists of surfactant and holes, a system which is isomorphic with an incompressible solution. Nearest neighbor pairs of chain monomers have interaction energies as follows: ϵ_{HH} and ϵ_{HT} and ϵ_{TT} , where the subscript H stands for the head group, while T denotes tail monomer. The energy of interaction of any species with a hole is identically zero. We utilized two interaction sets (I1)=(0,0,-2) and (I2)=(+2,+1,-2) where the interactions are given in the order (HH,HT,TT). The I2 interaction set [13] approximates more closely energetic interactions in nonionic surfactant solutions of the ethoxylated alkyl series. The surfactant molecules and the interaction sets studied are summarized in Table I. The reduced temperature, T^* , is defined with respect to the unit of interaction energies. An interesting point to note is that the exchange energy parameters, χ_{ij} , defined as

$$\chi_{ij} = \frac{1}{kT} \left[\epsilon_{ij} - \frac{\epsilon_{ii} + \epsilon_{jj}}{2} \right] \quad (2)$$

are the same for the HT and Th [h is an empty lattice position] in the two interaction sets. However, the χ_{HH} is more negative for the (I2) interaction set relative to (I1). In other words, although tails are repelled from holes and heads in the same manner in (I1) and (I2), (I2) has the additional factor that the heads are more strongly solubilized. Thus, these molecules will show a higher propensity to create nanostructures, rather than macroscopically phase separate.

We determined the phase coexistence of these solutions by the histogram reweighting method as described previously [6]. The micellization of these surfactant solutions were determined by monitoring the dependence of the osmotic pressure on composition. A relatively sudden decrease in the slope of this plot indicates either the formation of aggregates or phase separation as has been discussed previously [6]. For macroscopic phase separation, the slope after the break is a function of system size, decreasing to zero at the thermodynamic limit.

By contrast, for aggregating systems, the slope is independent of overall system size. Snapshots of the molecular positions, which are often used in simulation studies of aggregation can be misleading, indicating aggregation for systems that do not have stable, long-lived aggregates. Analysis of molecular configurations, however, provides information on the sizes and shapes of the aggregates.

B Some methodological issues

Given any reasonable definition for assigning two molecules to a single cluster, e.g. by asking that they are separated by less than a certain cutoff distance, one will always find aggregates in any solution. The question of how one determines whether such aggregates should be called micelles deserves some additional discussion. The size of a cluster is not a good indicator. After all, any system near a critical point for a first order phase transition shows formation of large clusters due to order parameter fluctuations. However, these clusters are weakly bound. Cluster size distributions show broad peaks, as there is no clearly preferred aggregation number. These distributions are also strong functions of overall concentration. Some recent simulation studies of aggregation [12] have been performed in this regime, because the low thermodynamic stability of the aggregates facilitates sampling of phase space.

By contrast, systems that form stable micellar aggregates that can be compared to experimentally observed micelles, have large free energy barriers separating the aggregated and free states. In our previous work [6] we have shown that for the surfactants H_3T_3 and H_4T_4 , we have “true” micelles only at low temperatures. As temperature is increased, the aggregates that form are less and less stable. We have, somewhat arbitrarily, set an upper limit for the slope of the osmotic pressure curves to separate “true” micellization from weak aggregation.

Finally, aggregation to large, stable clusters can be easily mistaken for a first-order transition in simulation studies of relatively small systems, as it is accompanied by hysteresis. However, the true thermodynamic character of a transition is easily revealed by performing

an analysis of the system size dependence of the transition location. In particular, except near critical points, the effect of system size on the location of a first-order transition is only minor. In contrast, for systems forming finite aggregates, there is a strong dependence of the apparent location of a transition. This can be understood as follows. Consider a surfactant system that preferentially forms aggregates of $N = 100$ molecules at very low concentrations of free molecules. Simulation in a system of volume $V = 1000$ will show a “phase” of mole fraction $N/V = 0.1$ corresponding to a single aggregate forming in the simulation cell. Doubling the system volume would not change the preferred aggregation number and thus the apparent transition will move to half the previous mole fraction. Thus, by examining the system size dependence of the location of (apparently) first order phase transition boundaries, we can reliably distinguish between micellization and macroscopic phase separation.

III. RESULTS

A Homopolymer Chains

Figure 1 shows phase diagrams for T chains of length 1 to 5 on a $z=26$ lattice. As expected, we find only liquid-vapor coexistence [or, isomorphically, coexistence between a T-rich and a T-lean phase]. Note that for chains of length $x = 4$, $T_c \approx 18$. To map the lattice chains lengths on to realistic alkanes in Figure 2 the volume fractions of T_x in the dilute phase are plotted as a function of inverse reduced temperature. Note that there are two unknowns at this juncture: these are the mapping of a lattice monomer to the corresponding number of monomers on a realistic chain, and the energy of interaction between two lattice monomers. The mole fractions are compared to experimental data for the solubility of normal alkanes in water from the correlations of Tsionopoulos [17], which are based on a critical evaluation of experimental measurements available for these systems. We find that utilizing $\epsilon = 60$ K and mapping two real monomers into a lattice model permits remarkably good agreement for the slope of the solubility curves at high temperature, and also for the length dependence of the solubility. Note that the experimental curves in Figure 2 were

scaled only along the temperature axis, and that the scaling of chain lengths then becomes apparent on visual inspection of the resulting figure. While this agreement is satisfactory, the deficiencies of the lattice model become apparent at lower temperatures, for which the solubility of hydrocarbons passes through a minimum. This solubility minimum is thought to be related to changes in the hydrogen-bonding structure of water. This fact cannot be captured by a solvent model with temperature independent interaction energies. The resulting real temperature scale is shown at the top of the graph.

B Role of Different Interaction Sets

We now proceed to examine the behavior of the surfactants and consider the (I1) interaction set. Phase separation is found for the molecules with the shortest heads, i.e., H_1T_4 (I1) and $T_2H_4T_2$ (I1). Figure 3 shows phase diagrams for H_1T_4 (I1) and $T_2H_4T_2$ (I1). Two different system sizes, $L=15$ (open symbols) and $L=10$ (filled symbols) are shown on the graph. The phase diagrams in Figure 3 do not depend on size, thus these are true phase transitions.

We now compare the behavior of the (I1) and (I2) interaction sets. We find that increasing the chain length of the H group or changing the interaction set from (I1) to (I2) has the consequence of facilitating nanostructure formation before phase separation [see Table I and Figures 4 and 5]. This is possible since either of these variations results in a dramatic lowering of the critical temperature, as expected. Note that, in Figures 4 and 5, the nanostructures which form are worm-like or cylindrical, suggesting that the Δ value lies between $1/2$ and $1/3$, which implies a large optimal area per head group, a_0 . Increasing the H length for (I2) to 2 groups then yields spherical micelles, which are characterized by an even smaller value of Δ [see Figure 6]. These results, in combination, suggest that as H group length is increased the Δ value decreases systematically. The transition from phase separation to worm-like micelles to spherical micelles happens in a quasi-continuous manner, stressing that the nanostructure formation is a subtle balance of solvophilic and solvophobic forces as noted above.

The critical micelle concentrations (cmc's) were determined with a slightly modified

methodology of [6]. Figure 7 illustrates the concept. The reduced osmotic pressure is obtained from the logarithm of the grand partition function, a quantity which can in turn be determined from the simulations to within an additive constant [6]. For the system H_2T_4 (I2), $L = 10$, we obtain the two curves shown on Figure 7 at the two temperatures indicated on the figure. There is a clear break indicating formation of aggregates. Instead of fitting the parts of the curve before and after the break to straight lines following [6], we have chosen to identify the cmc as the volume fraction of surfactant for which the second derivative of this curve is a maximum. The two definitions are essentially equivalent for the range of temperatures over which micellization is observed. In [6], it was demonstrated that this definition results in cmc's consistent with the macroscopic interpretation, namely as the concentration of surfactant for which the first well-defined micellar aggregate appears in solution. As temperature is increased, the change in slope of the osmotic pressure curves becomes more gradual and the break becomes less well-defined.

Figure 8 gives the cmc's, determined as the point at which the osmotic pressure curves have the maximum second derivative, for all surfactants studied that do not macroscopically phase separate. As the H chain length increases, the CMC is increased, in agreement to experimental observations for the polyoxyethylene nonionic surfactants [18]. Surfactants of the same architecture have generally higher cmc's for the (I2) interaction set, consistent with the observation earlier that the (I2) interaction set results in more hydrophilic interactions of the head groups. The triblock surfactants aggregate to micelles at much lower temperatures than the corresponding diblocks. This can be understood as a consequence of the much greater entropy loss for the two opposite hydrophobic blocks to come together.

Figure 9 shows the normalized cluster size distributions for the systems corresponding to Figures 5-6. For the H_2T_4 (I2) system, the distribution is almost perfectly Gaussian and the corresponding aggregates nearly spherical. For the H_1T_4 (I2) system, the distribution is much broader and has a long tail characteristic of cylindrical micelles. For the H_2T_4 (I1) system, there is an even broader distribution extending to aggregation numbers near 400. It is interesting to note that the next step in this progression is macroscopic phase separation. These distributions are qualitatively similar to those of [9], who have interpreted them as

resulting from a mixture of spherical and cylindrical micelles. The system of [9] was H_2T_2 surfactants on a face centered cubic lattice ($z = 12$) using the (I1) interaction set.

IV. DISCUSSION

The key result of the present work is the progression from macroscopic phase separation to formation of micellar aggregates at low concentrations for amphiphilic molecules as the surfactant architecture and interactions are varied. This progression is analogous to that seen experimentally, for example in the polyoxyethylene glycol monoether series, C_iE_j , with increasing hydrophilic segment length j . Our results show that only macroscopic phase separation occurs for surfactants in the case of short heads where the H group is athermal to the solvent. Situations where the heads are repelled appear not to phase separate for the T lengths examined. The propensity for microphase separation then reflects the opposite trend.

To try and place these results in perspective, we evoke the current state of the understanding of the related situation of block copolymer phase behavior, especially when the molecule is dissolved in a preferential solvent [19]. There are two relevant enthalpic parameters in this situation $\chi_{HT}zN, \chi_{sh}zN$. The first dimensionless group is relevant to the microphase separation of the surfactant, which occurs when this quantity increases above a threshold number. For long block copolymers, mean field theory suggests that this threshold value is 10.5. The second quantity, where χ_{sh} is the effective interaction parameter between a surfactant molecule and the holes, triggers phase separation. The Flory lattice model dictates that the critical value of this quantity is 2 for mixtures of long chain molecules. Note that both of these quantities, which will suggest the point where enthalpic interaction cause microphase or macrophase separation, scale linearly with z and N , the chain length of the surfactant.

Based on these ideas, then, we understand the complex behavior displayed by these surfactant molecules as follows. The pure T molecules only phase separate from solvent as expected. As one adds H moieties the propensity for phase mixing increases, since χ_{sh}

decreases. When one goes from the (I1) to (I2) sets, the χ_{sh} becomes smaller although the χ_{HT} stays unchanged. Thus, (I2) systems show lower propensity to phase separate, and hence a higher tendency to form micelles. These results are in qualitative agreement with simulation, but await quantitative treatment through the use of mean-field theories, such as the single chain theory of Szleifer [4]

A final point we note is the progression of structures for the (I2) interaction set with increasing length of the H block. For the shortest H block the system forms cylindrical micelles, while for longer H blocks they form spheres. These results may also be understood by seeking guidance from the nanostructures formed by block copolymers in selective solvents. The fact that the H_1T_4 (I2) molecule forms cylinders can be understood by realizing that this head block is strongly solubilized in solvent, since it strongly repels other H moieties. Thus, this solubilized block is effectively much longer justifying its cylindrical micellar geometry. A logical progression of these ideas suggests that the longer blocks can either form lamellae (at high overall volume fractions) or spheres (at low volume fractions). Consequently, all longer H blocks must result in spheres near the cmc, as is found.

In the present paper, we have focused on the solution behavior at low overall concentrations of surfactant. We have not investigated the formation of liquid crystalline phases at higher concentrations. The formation of lamellar phases has been used experimentally as a probe of the onset of order in solution as the length of the head and tail groups are varied [20].

V. CONCLUSIONS

We have found that the balance between phase separation and nanostructure formation is delicate in these surfactant molecules. Increasing the effective “dislike” between a surfactant molecule and the solvent always favors the formation of phase separated structures. The inverse correlation is found for micellization. The Monte Carlo simulations results presented here clearly illustrate that there is a gradual transition between macroscopic phase separation and micellization. Small changes can result in dramatic variations in the resulting

microstructures. As the length of the H groups increases we find a progression of nanostructures from worm-like micelles, to cylinders and finally spheres. These ideas are qualitatively consistent with notions derived from the block copolymer literature. These simulation results represent the first systematic efforts to understand these complex morphological transitions which occur at low concentrations for short-chain surfactant systems.

VI. ACKNOWLEDGEMENTS

This work was initiated at the University of Maryland, where funding was provided by the Department of Energy, Office of Basic Energy Sciences (DE-FG02-98ER14858) and by the Petroleum Research Fund administered by the American Chemical Society (grant 34164AC9). At Penn State, this research was funded by the National Science Foundation [CTS-9975625].

TABLE I: Surfactants architectures and interaction energy sets studied.

Molecule	I1	I2
T_x (x=1-4)	Phase separates	Phase separates
H_1T_4	Phase separates	Cylindrical micelles
H_2T_4	Worm-like micelles	Spherical Micelles
H_4T_4	Spherical micelles [6]	Spherical micelles
$T_2H_4T_2$	Phase separates	Spherical micelles
$T_2H_8T_2$	Spherical micelles	

REFERENCES

- [1] Israelachvili, J. *Intermolecular and Surface Forces*. Academic Press, London, (1992).
- [2] Ruckenstein, E. and Nagarajan, R. *J. Phys. Chem.* **85**, 3010 (1981).
- [3] Tanford, C. *The Hydrophobic Effect*. Wiley, New York, (1980).
- [4] Szleifer, I., Ben-Shaul, A., and Gelbart, W. M. *J Chem. Phys.* **83**, 2612 (1985).
- [5] Israelachvili, J., Mitchell, D., and Ninham, B. W. *J. Chem. Soc. Faraday Trans.* **72**, 1525 (1972).
- [6] Floriano, M. A., Caponetti, E., and Panagiotopoulos, A. Z. *Langmuir* **15**, 3143 (1999).
- [7] Kositzka, M. J., Bohne, C., Alexandridis, P., Hatton, T. A., and Holzwarth, J. F. *Macromolecules* **32**, 5539–51 (1999).
- [8] Smit, B., Hilbers, P., Esselink, K., L. A. Rupert, L., van Os, N. M., and Schlijper, A. G. *Nature* **348**, 624–5 (1990).
- [9] Nelson, P. H., Rutledge, G. C., and Hatton, T. A. *J. Chem. Phys.* **107**, 10777–81 (1997).
- [10] Xing, L. and Mattice, W. L. *Macromolecules* **30**, 1711–1717 (1997).
- [11] Viduna, D., Milchev, A., and Binder, K. *MACROMOL THEOR SIMUL.* **7**, 649–58 (1998).
- [12] Girardi, M. and Figueiredo, W. *J. Chem. Phys.* **112**, 4833–5 (2000).
- [13] Chatterjee, A. P. and Panagiotopoulos, A. Z. *in Computer Simulation Studies in Con-*

- densed Matter Physics*, D. P. Landau (ed.). Springer Proceeding in Physics vol. 85, pp. 211-222, (1999).
- [14] Larson, R. G., Scriven, L. E., and Davis, H. T. *J. Chem. Phys.* **83**, 2411–20 (1985).
- [15] Larson, R. G. *J. Chem. Phys.* **89**, 1642–50 (1988).
- [16] Larson, R. G. *J. Phys. II France* **6**, 1441–63 (1996).
- [17] Tsouopoulos, C. *Fluid Phase Equil.* **156**, 21 (1999).
- [18] Rosen, M. J. *Surfactants and Interfacial Phenomena*, 2nd Ed. John Wiley and Sons, New York, (1989).
- [19] Bates, F. S. and Fredrickson, G. H. *Ann Rev. Phys. Chem.* **41**, 525 (1990).
- [20] Koehler, R. D., Schubert, K.-V., Strey, R., and Kaler, E. W. *J. Chem. Phys.* **101**, 10843–9 (1994).

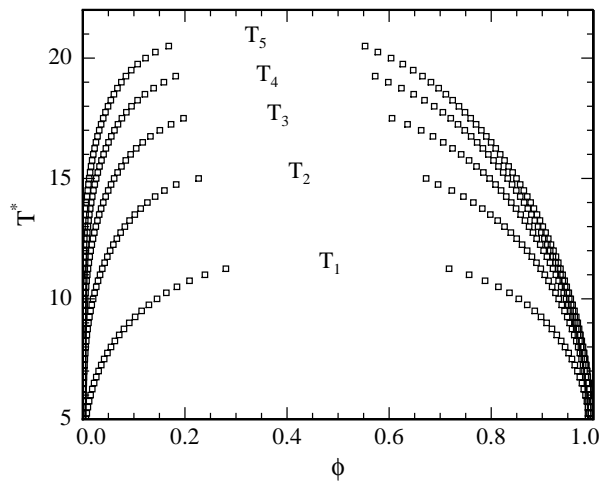


FIG. 1: Phase behavior of homopolymer chains of length 1 to 5.

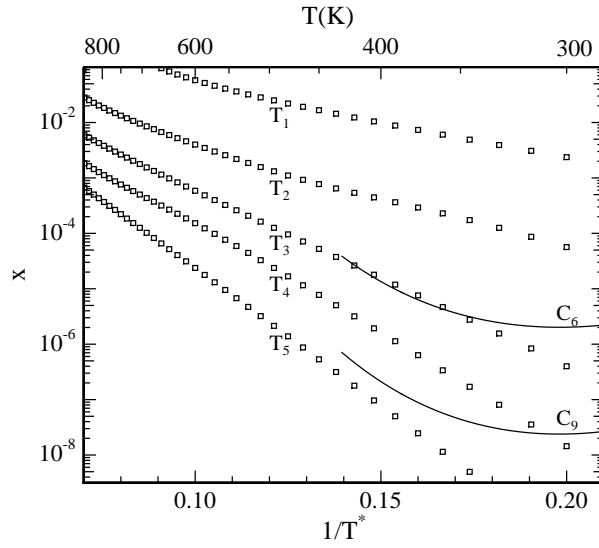


FIG. 2: Mole fraction in dilute phase versus the inverse reduced temperature for homopolymer chains of length 1 to 5 (points, top curve is $r=1$). The top scale gives the corresponding real temperature, assuming that $\epsilon=60$ K. Experimental data for n -hexane and n -nonane are shown as continuous lines (top curve is for n -hexane).

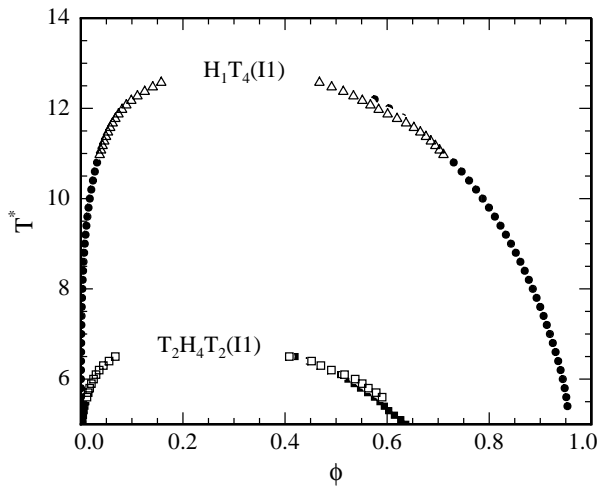


FIG. 3: Phase diagrams for amphiphiles that do not form micelles on the $z=26$ lattice

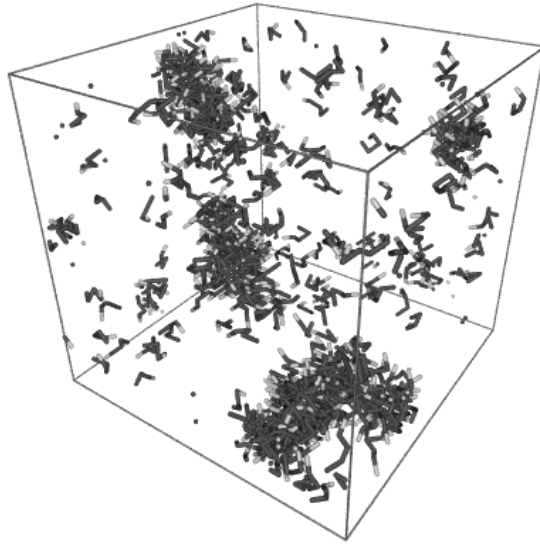


FIG. 4: Snapshot of the $H_1T_4(I_2)$, $L = 40$ system at $T^* = 8$, $\mu = -47.8$.

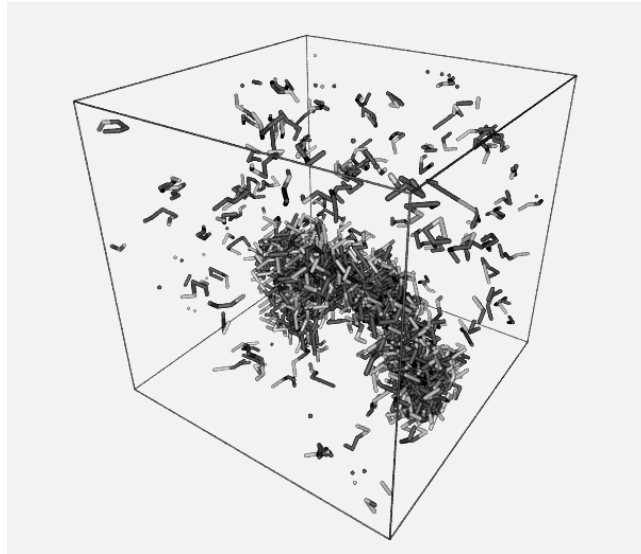


FIG. 5: Snapshot of the $H_2T_4(I_1)$, $L = 40$ system at $T^* = 8$, $\mu = -51.4$.

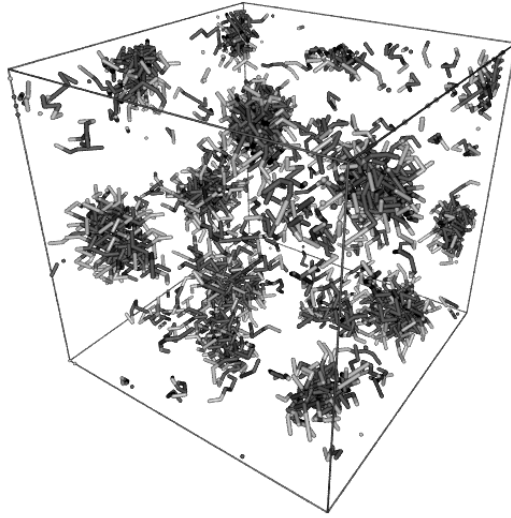


FIG. 6: Snapshot of the $\text{H}_2\text{T}_4(\text{I}2)$, $L = 40$ system at $T^* = 7$, $\mu = -40.3$.

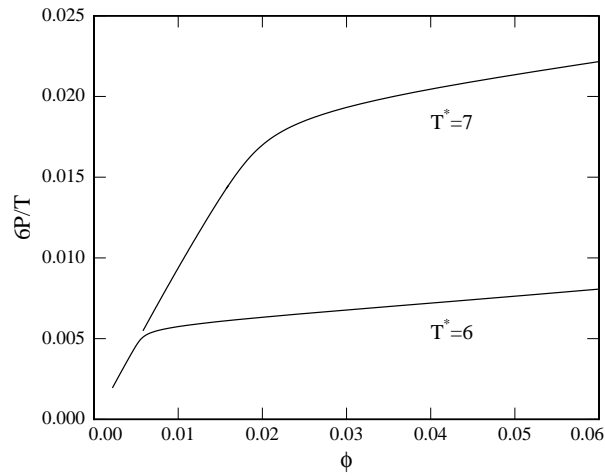


FIG. 7: Reduced osmotic pressure, $6P^*/T^*$ versus volume fraction of surfactant for the $\text{H}_2\text{T}_4(\text{I}2)$ system, $L = 10$.

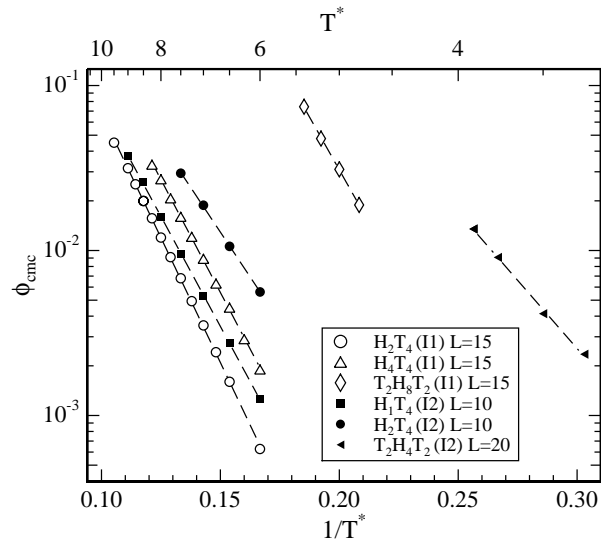


FIG. 8: The critical micelle concentration, ϕ_{cmc} plotted against inverse temperature for all systems that form micelles.

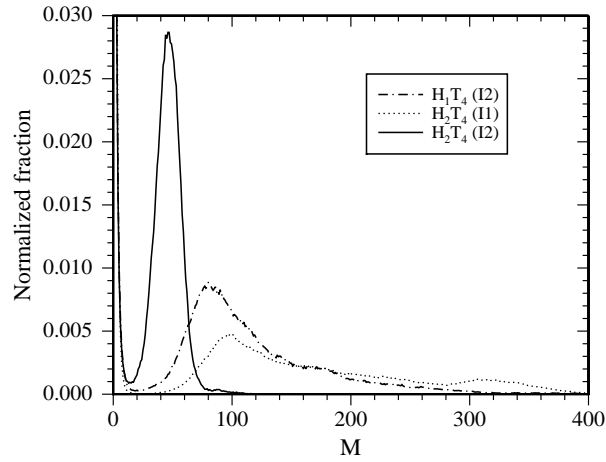


FIG. 9: Normalized cluster probability distributions corresponding to figures 4 - 6 respectively.